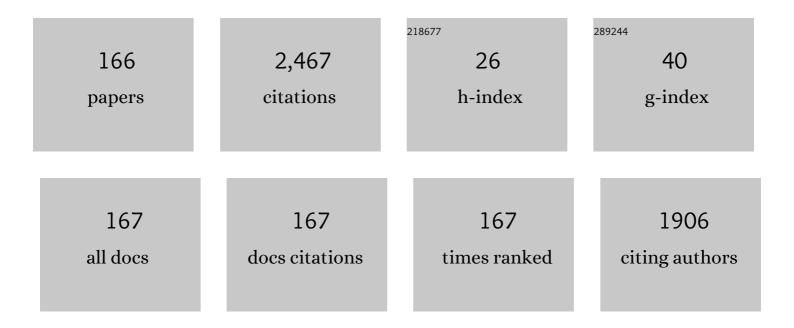
Tetsuo Uchikoshi

List of Publications by Year in descending order

Source: https://exaly.com/author-pdf/9023109/publications.pdf Version: 2024-02-01



#	Article	IF	CITATIONS
1	Video Processing Electrophoretic Measurements under High Electric Fields for Sub-millimeter Particles in Oil. Journal of Oleo Science, 2022, 71, 445-457.	1.4	1
2	Light-dependent ionic-electronic conduction in an amorphous octahedral molybdenum cluster thin film. NPG Asia Materials, 2022, 14, .	7.9	11
3	Effect of CNT addition and its orientation on thermal shock resistance of B ₄ C/CNT composites fabricated by hot-pressing. Journal of Asian Ceramic Societies, 2022, 10, 370-377.	2.3	2
4	Two-step electrochemical deposition of Ni(OH)2/FeOOH bilayer electrocatalyst for oxygen evolution reaction. Materials Letters, 2022, 317, 132118.	2.6	5
5	Evidence of the Ambipolar Behavior of Mo ₆ Cluster Iodides in All-Inorganic Solar Cells: A New Example of Nanoarchitectonic Concept. ACS Applied Materials & Interfaces, 2022, 14, 1347-1354.	8.0	19
6	Nanoarchitectonics of Glass Coatings for Near-Infrared Shielding: From Solid-State Cluster-Based Niobium Chlorides to the Shaping of Nanocomposite Films. ACS Applied Materials & Interfaces, 2022, 14, 21116-21130.	8.0	4
7	Material Texture and α-β Phase Transition of Self-assembled BaTiO ₃ /Polyvinylidene Fluoride Composites. Funtai Oyobi Fummatsu Yakin/Journal of the Japan Society of Powder and Powder Metallurgy, 2022, 69, 195-199.	0.2	3
8	Fabrication and characterization of zeolite bulk body containing mesopores and macropores using starch as pore-forming agent. Advanced Powder Technology, 2022, 33, 103626.	4.1	5
9	Controlling the Deposition Process of Nanoarchitectonic Nanocomposites Based on {Nb6â^xTaxXi12}n+ Octahedral Cluster-Based Building Blocks (Xi = Cl, Br; 0 ≤ ≤6, n = 2, 3, 4) for UV-NIR Blockers Coating Applications. Nanomaterials, 2022, 12, 2052.	4.1	3
10	Hafnium Oxide Nanostructured Thin Films: Electrophoretic Deposition Process and DUV Photolithography Patterning. Nanomaterials, 2022, 12, 2334.	4.1	4
11	Fabrication of textured B4C ceramics with oriented tubal pores by strong magnetic field-assisted colloidal processing. Journal of the European Ceramic Society, 2021, 41, 2366-2374.	5.7	4
12	Fabrication of BSCF-based mixed oxide ionic-electronic conducting multi-layered membrane by sequential electrophoretic deposition process. Journal of the European Ceramic Society, 2021, 41, 2709-2715.	5.7	10
13	Revisiting properties of edge-bridged bromide tantalum clusters in the solid-state, in solution and vice versa: an intertwined experimental and modelling approach. Dalton Transactions, 2021, 50, 8002-8016.	3.3	11
14	Development of novel boneâ€like nanocomposite coating of hydroxyapatite/collagen on titanium by modified electrophoretic deposition. Journal of Biomedical Materials Research - Part A, 2021, 109, 1905-1911.	4.0	13
15	Microstructure Control of Ceramic Functional Membrane by Electrophoretic Deposition Method and Its Application to Oxygen Separation Membrane using Mixed Ionic-Electronic Conductor. Funtai Oyobi Fummatsu Yakin/Journal of the Japan Society of Powder and Powder Metallurgy, 2021, 68, 121-128.	0.2	0
16	Production of crystal-oriented lanthanum silicate oxyapatite ceramics with anisotropic electrical conductivity and thermal expansion. Open Ceramics, 2021, 6, 100100.	2.0	3
17	Solutionâ€Based Approach for the Continuous Fabrication of Thin Lithiumâ€Ion Battery Electrodes by Wet Mechanochemical Synthesis and Electrophoretic Deposition. Advanced Engineering Materials, 2021, 23, 2100524.	3.5	4
18	Robust, Transparent Hybrid Thin Films of Phase-Change Material Sb ₂ S ₃ Prepared by Electrophoretic Deposition. ACS Applied Energy Materials, 2021, 4, 9891-9901.	5.1	15

#	Article	IF	CITATIONS
19	Antibacterial-functionalized Ag loaded-hydroxyapatite (HAp) coatings fabricated by electrophoretic deposition (EPD) process. Materials Letters, 2021, 297, 129955.	2.6	3
20	Sequenced Successive Ionic Layer Adsorption and Reaction for Rational Design of Ni(OH)2/FeOOH Heterostructures with Tailored Catalytic Properties. ACS Applied Energy Materials, 2021, 4, 8252-8261.	5.1	6
21	Synthesis of novel hexamolybdenum cluster-functionalized copper hydroxide nanocomposites and its catalytic activity for organic molecule degradation. Science and Technology of Advanced Materials, 2021, 22, 758-771.	6.1	3
22	Effect of crystalline orientation on photocatalytic performance for Nb-doped TiO2 nanoparticles. Advanced Powder Technology, 2021, 32, 4149-4154.	4.1	5
23	Shell-thickness control of hollow SiO2 nanoparticles through post-treatment using sol–gel technique toward efficient water confinement. Colloids and Surfaces A: Physicochemical and Engineering Aspects, 2021, 629, 127501.	4.7	2
24	Effect of Aâ€site ion nonstoichiometry on the chemical stability and electric conductivity of strontium and magnesiumâ€doped lanthanum gallate. Journal of the American Ceramic Society, 2020, 103, 790-799.	3.8	4
25	Nest-like microstructured biocompatible membrane fabricated by hydrothermally-synthesized hydroxyapatite (HAp) whiskers. Journal of the European Ceramic Society, 2020, 40, 513-520.	5.7	9
26	Solution-mediated nanometric growth of α-Fe ₂ O ₃ with electrocatalytic activity for water oxidation. Nanoscale Advances, 2020, 2, 3933-3941.	4.6	3
27	Electrophoretically Deposited Layers of Octahedral Molybdenum Cluster Complexes: A Promising Coating for Mitigation of Pathogenic Bacterial Biofilms under Blue Light. ACS Applied Materials & Interfaces, 2020, 12, 52492-52499.	8.0	23
28	Zn-Al layered double hydroxide-based nanocomposite functionalized with an octahedral molybdenum cluster exhibiting prominent photoactive and oxidation properties. Applied Clay Science, 2020, 196, 105765.	5.2	16
29	Effect of Surface Modification with TiO2 Coating on Improving Filtration Efficiency of Whisker-Hydroxyapatite (HAp) Membrane. Coatings, 2020, 10, 670.	2.6	6
30	Fabrication of polystyrene colloidal crystal film by electrophoretic deposition. Advanced Powder Technology, 2020, 31, 3085-3092.	4.1	13
31	Robust Structurally Colored Coatings Composed of Colloidal Arrays Prepared by the Cathodic Electrophoretic Deposition Method with Metal Cation Additives. ACS Applied Materials & Interfaces, 2020, 12, 40768-40777.	8.0	12
32	Rapid Growth of Colloidal Crystal Films from the Concentrated Aqueous Ethanol Suspension. Langmuir, 2020, 36, 10683-10689.	3.5	6
33	Zn–Al Layered Double Hydroxide Film Functionalized by a Luminescent Octahedral Molybdenum Cluster: Ultraviolet–Visible Photoconductivity Response. ACS Applied Materials & Interfaces, 2020, 12, 40495-40509.	8.0	15
34	Original Synthesis of Molybdenum Nitrides Using Metal Cluster Compounds as Precursors: Applications in Heterogeneous Catalysis. Chemistry of Materials, 2020, 32, 6026-6034.	6.7	11
35	Fabrication of porous (Ba,Sr)(Co,Fe)O3-Ĩ´ (BSCF) ceramics using gelatinization and retrogradation phenomena of starch as pore-forming agent. Ceramics International, 2020, 46, 13047-13053.	4.8	16
36	Synthesis of Euâ€doped hydroxyapatite whiskers and fabrication of phosphor layer via electrophoretic deposition process. Journal of the American Ceramic Society, 2020, 103, 6780-6792.	3.8	6

#	Article	IF	CITATIONS
37	Significantly improved photoluminescence of the greenâ€emitting βâ€sialon:Eu ²⁺ phosphor via surface coating of TiO ₂ . Journal of the American Ceramic Society, 2019, 102, 294-302.	3.8	5
38	Fabrication of BSCF-based mixed ionic-electronic conducting membrane by electrophoretic deposition for oxygen separation application. Journal of the European Ceramic Society, 2019, 39, 5292-5297.	5.7	9
39	Controllable Design of Various Microstructures for Hydroxyapatite Coatings by Electrophoresis Deposition Process for Biomedical Applications. Journal of the Electrochemical Society, 2019, 166, D700-D706.	2.9	5
40	Effect of Al2O3 addition on texturing in a rotating strong magnetic field and densification of B4C. Ceramics International, 2019, 45, 18222-18228.	4.8	12
41	Transparent functional nanocomposite films based on octahedral metal clusters: synthesis by electrophoretic deposition process and characterization. Royal Society Open Science, 2019, 6, 181647.	2.4	13
42	Surface Modification on Cellulose Nanofibers by TiO2 Coating for Achieving High Capture Efficiency of Nanoparticles. Coatings, 2019, 9, 139.	2.6	9
43	Anisotropic Electric Conductivity and Battery Performance in <i>C</i> -axis Oriented Lanthanum Silicate Oxyapatite Prepared by Slip Casting in a Strong Magnetic Field. Materials Transactions, 2019, 60, 1949-1953.	1.2	5
44	Rapid Fabrication of Colloidal Crystal Films by Electrophoretic Deposition and Its Application for a Volatile Liquid and Strain Detection Sensor. Journal of the Society of Powder Technology, Japan, 2019, 56, 339-346.	0.1	2
45	Fabrication of lead-free piezoelectric (Bi0.5Na0.5)TiO3–BaTiO3 ceramics using electrophoretic deposition. Journal of Materials Science, 2018, 53, 2396-2404.	3.7	14
46	Observation of stacking faults and photoluminescence of laurate ion intercalated Zn/Al layered double hydroxide. Materials Letters, 2018, 213, 323-325.	2.6	8
47	Anisotropic Electronic Conductivity and Battery Performance in C-axis Oriented Lanthanum Silicate Oxyapatite Prepared by Slip Casting in a Strong Magnetic Field. Funtai Oyobi Fummatsu Yakin/Journal of the Japan Society of Powder and Powder Metallurgy, 2018, 65, 121-126.	0.2	0
48	Preparation of textured B ₄ C compact with oriented pore-forming agent by slip casting under strong magnetic field. Journal of the Ceramic Society of Japan, 2018, 126, 832-838.	1.1	3
49	Extended Study on Electrophoretic Deposition Process of Inorganic Octahedral Metal Clusters: Advanced Multifunctional Transparent Nanocomposite Thin Films. Bulletin of the Chemical Society of Japan, 2018, 91, 1763-1774.	3.2	26
50	Embedding hexanuclear tantalum bromide cluster {Ta6Br12} into SiO2 nanoparticles by reverse microemulsion method. Heliyon, 2018, 4, e00654.	3.2	9
51	Effect of ball-milling time and surfactant content for fabrication of 0.85(Bi _{0.5} Na _{0.5})TiO ₃ :0.15BaTiO <sub& green ceramics by electrophoretic deposition. Journal of the Ceramic Society of Japan, 2018, 126, 542-546.</sub& 	gt;31.1	սbֆgt;
52	New ultra-violet and near-infrared blocking filters for energy saving applications: fabrication of tantalum metal atom cluster-based nanocomposite thin films by electrophoretic deposition. Journal of Materials Chemistry C, 2017, 5, 10477-10484.	5.5	41
53	Mo ₆ cluster-based compounds for energy conversion applications: comparative study of photoluminescence and cathodoluminescence. Science and Technology of Advanced Materials, 2017, 18, 458-466.	6.1	37
54	Magnetic properties of α″-Fe16N2-like compound derived from Fe3O4 fine powder coated on hard magnetic BaFe12O19 particles. Journal of Magnetism and Magnetic Materials, 2017, 443, 73-78.	2.3	3

#	Article	IF	CITATIONS
55	Colloidal processing of Li ₂ S–P ₂ S ₅ films fabricated via electrophoretic deposition methods and their characterization as a solid electrolyte for all solid state lithium ion batteries. Journal of the Ceramic Society of Japan, 2017, 125, 287-292.	1.1	10
56	Electrophoretic Coating of Octahedral Molybdenum Metal Clusters for UV/NIR Light Screening. Coatings, 2017, 7, 114.	2.6	13
57	Electrophoretic fabrication of a-b plane oriented La2NiO4 cathode onto electrolyte in strong magnetic field for low-temperature operating solid oxide fuel cell. Journal of the European Ceramic Society, 2016, 36, 4077-4082.	5.7	19
58	Triaxial Crystalline Orientation of MgTi ₂ O ₅ Achieved Using a Strong Magnetic Field and Geometric Effect. Journal of the American Ceramic Society, 2016, 99, 1852-1854.	3.8	7
59	Prevention of thermal- and moisture-induced degradation of the photoluminescence properties of the Sr ₂ Si ₅ N ₈ :Eu ²⁺ red phosphor by thermal post-treatment in N ₂ –H ₂ . Physical Chemistry Chemical Physics, 2016, 18, 12494-12504.	2.8	36
60	Inorganic Molybdenum Clusters as Lightâ€Harvester in All Inorganic Solar Cells: A Proof of Concept. ChemistrySelect, 2016, 1, 2284-2289.	1.5	35
61	Visible tunable lighting system based on polymer composites embedding ZnO and metallic clusters: from colloids to thin films. Science and Technology of Advanced Materials, 2016, 17, 443-453.	6.1	25
62	Sinterable powder fabrication of lanthanum silicate oxyapatite based on solid-state reaction method. Journal of the Ceramic Society of Japan, 2015, 123, 274-279.	1.1	8
63	Fabrication of (111)-oriented Tetragonal BaTiO ₃ Ceramics by an Electrophoretic Deposition in a High Magnetic Field. Transactions of the Materials Research Society of Japan, 2015, 40, 223-226.	0.2	8
64	Influence of the crystal structure on the physical properties of monoclinic ZrO 2 nanocrystals. Nano Structures Nano Objects, 2015, 1, 1-6.	3.5	3
65	Reduced thermal degradation of the red-emitting Sr ₂ Si ₅ N ₈ :Eu ²⁺ phosphor via thermal treatment in nitrogen. Journal of Materials Chemistry C, 2015, 3, 7642-7651.	5.5	60
66	Effect of Electrode Reactions during Aqueous Electrophoretic Deposition on Bulk Suspension Properties and Deposition Quality. Key Engineering Materials, 2015, 654, 3-9.	0.4	7
67	UV Protection Mechanism and Property of Functional Ceramic Particles. Hyomen Kagaku, 2014, 35, 45-49.	0.0	0
68	Phosphor Deposits of β-Sialon:Eu2+ Mixed with SnO2 Nanoparticles Fabricated by the Electrophoretic Deposition (EPD) Process. Materials, 2014, 7, 3623-3633.	2.9	11
69	Crystalline-Oriented Beta-Sialon:Eu2+Deposits Fabricated by Electrophoretic Deposition (EPD) within Strong Magnetic Field. ECS Journal of Solid State Science and Technology, 2014, 3, R195-R199.	1.8	2
70	Interaction between A-site deficient La0.8Sr0.2Ga0.8Mg0.2O3â^'δ (LSGM8282) and Ce0.9Gd0.1O3â^'δ (GDC) electrolytes. Solid State Ionics, 2014, 258, 18-23.	2.7	6
71	Beta-sialon phosphor deposits fabricated by electrophoretic deposition (EPD) process in a magnetic field. Ceramics International, 2014, 40, 8369-8375.	4.8	11
72	Positional-dependent luminescence property of β-SiAlON:Eu2+ phosphor particle. Applied Physics Letters, 2014, 104, .	3.3	8

#	Article	IF	CITATIONS
73	Magnesium ion distribution and defect concentrations of MgO-doped lanthanum silicate oxyapatite. Solid State Ionics, 2014, 258, 24-29.	2.7	4
74	Grain orientation of Nd-modified bismuth titanate ceramics by forming at low magnetic field. Journal of the Ceramic Society of Japan, 2014, 122, 58-62.	1.1	3
75	Fabrication of Textured Ceramics Using Mn and Nb-doped Hexagonal BaTiO ₃ by an Electrophoretic Deposition in a High Magnetic Field. Transactions of the Materials Research Society of Japan, 2014, 39, 199-202.	0.2	1
76	Surface modification of Ca-α-SiAlON: Eu2+ phosphor particles by SiO2 coating and fabrication of its deposit by electrophoretic deposition (EPD) process. Applied Surface Science, 2013, 280, 229-234.	6.1	28
77	The Characteristic of Inner Surface Coating on Porous Al ₂ O ₃ Tube by Electrophoretic Deposition. Key Engineering Materials, 2013, 545, 19-23.	0.4	1
78	Twoâ€Dimensional Orientation in <scp><scp>Bi</scp></scp> ₄ <scp><tcp>Ti</tcp></scp> ₃ <scp><scp>O</scp><!--<br-->Prepared Using Platelet Particles and a Magnetic Field. Journal of the American Ceramic Society, 2013, 96, 1085-1089.</scp>	sub>12 <td>subz</td>	subz
79	Ideal design of textured LiCoO2 sintered electrode for Li-ion secondary battery. APL Materials, 2013, 1, .	5.1	20
80	pH localization: a case study during electrophoretic deposition of ternary MAX phase carbide-Ti ₃ SiC ₂ . Journal of the Ceramic Society of Japan, 2013, 121, 348-354.	1.1	23
81	Electrophoretic deposition of orientation-controlled zeolite L layer on porous ceramic substrate. Journal of the Ceramic Society of Japan, 2013, 121, 370-372.	1.1	5
82	Hydrothermal transformation of magnetically orientation-controlled seed layer into orientation-retained dense, continuous film in clear reaction solution. Journal of the Ceramic Society of Japan, 2013, 121, 550-554.	1.1	1
83	Fabrication of textured α-alumina in high magnetic field via gelcasting with the use of glucose derivative. Journal of the Ceramic Society of Japan, 2013, 121, 89-94.	1.1	7
84	Fabrication of Textured BaTiO ₃ Ceramics by Electrophoretic Deposition in A High Magnetic Field using Single-domain Particles. Transactions of the Materials Research Society of Japan, 2013, 38, 41-44.	0.2	4
85	Orientation Control of Hematite via Transformation of Textured Goethite Prepared by EPD in a Strong Magnetic Field. Key Engineering Materials, 2012, 507, 227-231.	0.4	1
86	Textured Ti ₃ SiC ₂ by gelcasting in a strong magnetic field. Journal of the Ceramic Society of Japan, 2012, 120, 544-547.	1.1	11
87	Fabrication and Analysis of the Oriented <scp><scp>LiCoO</scp></scp> ₂ by Slip Casting in a Strong Magnetic Field. Journal of the American Ceramic Society, 2012, 95, 3428-3433.	3.8	11
88	Electrophoretic Deposition of <scp><scp>Ti</scp></scp> ₃ <scp><scp>SiC</scp>₂ and Texture Development in a Strong Magnetic Field. Journal of the American Ceramic Society, 2012, 95, 2857-2862.</scp>	3.8	27
89	Optical and adhesive properties of composite silica-impregnated Ca-α-SiAlON:Eu2+ phosphor films prepared on silica glass substrates. Journal of the European Ceramic Society, 2012, 32, 1365-1369.	5.7	7
90	Influence of niobium doping on phase composition and defect-mediated photoluminescence properties of Eu3+-doped TiO2 nanopowders synthesized in Ar/O2 thermal plasma. Journal of Alloys and Compounds, 2011, 509, 8944-8951.	5.5	5

#	Article	IF	CITATIONS
91	Texture development in anatase and rutile prepared by slip casting in a strong magnetic field. Journal of the Ceramic Society of Japan, 2011, 119, 334-337.	1.1	13
92	Texture development of surface-modified SiC prepared by EPD in a strong magnetic field. Journal of the Ceramic Society of Japan, 2011, 119, 667-671.	1.1	4
93	Preparation and Characterization of Grain-Oriented Barium Titanate Ceramics Using Electrophoresis Deposition Method under a High Magnetic Field. Key Engineering Materials, 2011, 485, 313-316.	0.4	4
94	High-concentration niobium (V) doping into TiO ₂ nanoparticles synthesized by thermal plasma processing. Journal of Materials Research, 2011, 26, 658-671.	2.6	17
95	Microstructure Control of Barium Titanate – Potassium Niobate Solid Solution System Ceramics by MPB Engineering and their Piezoelectric Properties. Key Engineering Materials, 2011, 485, 89-92.	0.4	9
96	Emission color tuning of laminated and mixed SiAlON phosphor films by electrophoretic deposition. Journal of the Ceramic Society of Japan, 2010, 118, 1-4.	1.1	20
97	Fabrication of c-axis oriented zinc oxide by electrophoretic deposition in a rotating magnetic field. Journal of the European Ceramic Society, 2010, 30, 1171-1175.	5.7	13
98	Experimental verification of pH localization mechanism of particle consolidation at the electrode/solution interface and its application to pulsed DC electrophoretic deposition (EPD). Journal of the European Ceramic Society, 2010, 30, 1187-1193.	5.7	70
99	Forming and Microstructure Control of Ceramics by Electrophoretic Deposition (EPD). KONA Powder and Particle Journal, 2010, 28, 74-90.	1.7	31
100	Electrophretic Deposition of LDC/LSGM/LDC Tri-layers on NiO-YSZ for Anode-supported SOFC. Transactions of the Materials Research Society of Japan, 2010, 35, 723-725.	0.2	2
101	Enhanced Piezoelectric Properties of Barium Titanate-Potassium Niobate Solid Solution System Ceramics by MPB Engineering. Key Engineering Materials, 2010, 445, 11-14.	0.4	9
102	Synthesis, Microstructure and Mechanical Properties of ZrB ₂ Ceramic Prepared by Mechanical Alloying and Spark Plasma Sintering. Key Engineering Materials, 2010, 434-435, 165-168.	0.4	1
103	Sedimentation classification treatment effect of starting powders in slip casting on magneto-orientation of mordenite zeolite. Transactions of the Materials Research Society of Japan, 2010, 35, 701-703.	0.2	2
104	Magnetic orientation and magnetic anisotropy in paramagnetic layered oxides containing rare-earth ions. Science and Technology of Advanced Materials, 2009, 10, 014604.	6.1	35
105	Photoanode characteristics of dye-sensitized solar cell containing TiO2 layers with different crystalline orientations. Journal of Materials Research, 2009, 24, 1417-1421.	2.6	8
106	Formation of Crystalline-Oriented Titania Thin Films on ITO Glass Electrodes by EPD in a Strong Magnetic Field. Key Engineering Materials, 2009, 412, 143-148.	0.4	2
107	Fabrication of Multi-Layered Thermoelectric Thick Films and their Thermoelectric Performance. Key Engineering Materials, 2009, 412, 291-296.	0.4	0
108	Preparation of Crystallineâ€Oriented Titania Photoelectrodes on ITO Glasses from a 2â€Propanol–2,4â€Pentanedione Solvent by Electrophoretic Deposition in a Strong Magnetic Field. Journal of the American Ceramic Society, 2009, 92, 984-989.	3.8	25

#	Article	IF	CITATIONS
109	Effect of bead-milling treatment on the dispersion of tetragonal zirconia nanopowder and improvements of two-step sintering. Journal of the Ceramic Society of Japan, 2009, 117, 470-474.	1.1	13
110	Fabrication of GDC/LSGM/GDC tri-layers on polypyrrole-coated NiO-YSZ by electrophoretic deposition for anode-supported SOFC. Journal of the Ceramic Society of Japan, 2009, 117, 1246-1248.	1.1	20
111	Fabrication and some properties of textured alumina-related compounds by colloidal processing in high-magnetic field and sintering. Journal of the European Ceramic Society, 2008, 28, 935-942.	5.7	55
112	Highly Texturing β-Sialon Via Strong Magnetic Field Alignment. Journal of the American Ceramic Society, 2008, 91, 620-623.	3.8	15
113	Conductive Polymer Coating on Nonconductive Ceramic Substrates for Use in the Electrophoretic Deposition Process. Journal of the American Ceramic Society, 2008, 91, 1674-1677.	3.8	26
114	Phosphate Esters as Dispersants for the Cathodic Electrophoretic Deposition of Alumina Suspensions. Journal of the American Ceramic Society, 2008, 91, 1923-1926.	3.8	20
115	Bubbleâ€Free Aqueous Electrophoretic Deposition (EPD) by Pulseâ€Potential Application. Journal of the American Ceramic Society, 2008, 91, 3154-3159.	3.8	68
116	Texturing of Si ₃ N ₄ Ceramics via Strong Magnetic Field Alignment. Key Engineering Materials, 2008, 368-372, 871-874.	0.4	6
117	Electrophoretic deposition of Eu2+ doped CaALPHASiAlON phosphor particles for packaging of flat pseudo-white light emitting devices. Journal of the Ceramic Society of Japan, 2008, 116, 740-743.	1.1	13
118	Grain-Orientation Control of Bi ₅ FeTi ₃ O ₁₅ Ceramics Prepared by Magnetic-Field-Assisted Electrophoretic Deposition Method. Key Engineering Materials, 2008, 388, 205-208.	0.4	1
119	Enhanced piezoelectric properties of grain-oriented Bi4Ti3O12–BaBi4Ti4O15 ceramics obtained by magnetic-field-assisted electrophoretic deposition method. Journal of Applied Physics, 2008, 104, .	2.5	19
120	Thermoelectric Properties and Magnetic Anisotropies of Magnetically Grain-Oriented Sr- or Bi-doped Ca3Co4O9 Thick Films. Materials Research Society Symposia Proceedings, 2007, 1044, 1.	0.1	0
121	Aqueous Processing of Textured Silicon Nitride Ceramics by Slip Casting in a Strong Magnetic Field. Materials Science Forum, 2007, 534-536, 1009-1012.	0.3	3
122	Improvement of Thermoelectric Properties of p- and n-types Oxide Thick Films Fabricated by Electrophoretic Deposition. Materials Research Society Symposia Proceedings, 2007, 1044, 1.	0.1	0
123	Hydrogen Storage Properties of Nb-Zr-Fe Alloys Disintegrated by Hydrogen Gas. Materials Science Forum, 2007, 534-536, 73-76.	0.3	0
124	Direct Shaping of Alumina Ceramics by Electrophoretic Deposition Using Conductive Polymer-Coated Ceramic Substrates. Advanced Materials Research, 2007, 29-30, 227-230.	0.3	2
125	Fabrication and Some Properties of Textured Ceramics by Colloidal Processing in High Magnetic Field. Key Engineering Materials, 2007, 352, 101-106.	0.4	3
126	Orientation Control in Multilayered Alumina Prepared Using Electrophoretic Deposition in a Strong Magnetic Field. Advanced Materials Research, 2007, 29-30, 223-226.	0.3	1

#	Article	IF	CITATIONS
127	Fabrication of Textured α-SiC Using Colloidal Processing and a Strong Magnetic Field. Materials Transactions, 2007, 48, 2883-2887.	1.2	20
128	Texturing CaALPHASialon Via Strong Magnetic Field Alignment. Journal of the Ceramic Society of Japan, 2007, 115, 701-705.	1.1	6
129	Synthesis of Titania Thin Films by Cathodic Electrolytic Deposition. Journal of the Ceramic Society of Japan, 2007, 115, 818-820.	1.1	3
130	Effect of Polyethylenimine on Hydrolysis and Dispersion Properties of Aqueous Si3N4Suspensions. Journal of the American Ceramic Society, 2007, 90, 797-804.	3.8	46
131	Electrophoretic Deposition of Alumina on Conductive Polymer-Coated Ceramic Substrates. Journal of the Ceramic Society of Japan, 2006, 114, 55-58.	1.3	19
132	Texture Development in Si3N4 Ceramics by Magnetic Field Alignment during Slip Casting. Journal of the Ceramic Society of Japan, 2006, 114, 979-987.	1.3	40
133	Texture Development in Alumina Composites by Slip Casting in a Strong Magnetic Field. Journal of the Ceramic Society of Japan, 2006, 114, 59-62.	1.3	22
134	Effect of polyethylenimine on the dispersion and electrophoretic deposition of nano-sized titania aqueous suspensions. Journal of the European Ceramic Society, 2006, 26, 1555-1560.	5.7	124
135	Mechanical properties of textured, multilayered alumina produced using electrophoretic deposition in a strong magnetic field. Journal of the European Ceramic Society, 2006, 26, 661-665.	5.7	30
136	Control of texture in alumina by colloidal processing in a strong magnetic field. Science and Technology of Advanced Materials, 2006, 7, 356-364.	6.1	106
137	Control of crystalline texture in polycrystalline TiO2 (Anatase) by electrophoretic deposition in a strong magnetic field. Journal of the European Ceramic Society, 2006, 26, 559-563.	5.7	49
138	Design of Alumina/Alumina Laminate Composites with Crystalline-Orientated Layers Produced by Electrophoretic Deposition under a High Magnetic Field. Key Engineering Materials, 2006, 314, 25-32.	0.4	0
139	Mechanical Properties of Textured Alumina Prepared by Colloidal Processing in a Strong Magnetic Field. Materials Research Society Symposia Proceedings, 2006, 977, 1.	0.1	0
140	Fabrication of multilayered oxide thermoelectric modules by electrophoretic deposition under high magnetic fields. Applied Physics Letters, 2006, 89, 081912.	3.3	30
141	Dispersion of SiC Suspensions with Cationic Dispersant of Polyethylenimine. Journal of the Ceramic Society of Japan, 2005, 113, 584-587.	1.3	15
142	Electrophoretic deposition of lead zirconate titanate (PZT) powder from ethanol suspension prepared with phosphate ester. Science and Technology of Advanced Materials, 2005, 6, 927-932.	6.1	37
143	Fabrication of porous ceramics with controlled pore size by colloidal processing. Science and Technology of Advanced Materials, 2005, 6, 915-920.	6.1	49
144	Alignment of TiO2 particles by electrophoretic deposition in a high magnetic field. Materials Research Bulletin, 2004, 39, 2155-2161.	5.2	17

#	Article	IF	CITATIONS
145	Electrophoretic deposition of alumina suspension in a strong magnetic field. Journal of the European Ceramic Society, 2004, 24, 225-229.	5.7	55
146	Electrophoretic deposition of aqueous nano-sized zinc oxide suspensions on a zinc electrode. Materials Research Bulletin, 2003, 38, 207-212.	5.2	46
147	Electrophoretic deposition of α-alumina particles in a strong magnetic field. Journal of Materials Research, 2003, 18, 254-256.	2.6	29
148	Stabilization of Yttria Aqueous Suspension with Polyethylenimine and Electrophoretic Deposition Journal of the Ceramic Society of Japan, 2002, 110, 840-843.	1.3	21
149	Electrical Conductivity of a 3Y-TZP/Alumina Laminate Composite Synthesized by Electrophoretic Deposition Journal of the Ceramic Society of Japan, 2002, 110, 959-962.	1.3	6
150	Electrophoretic Deposition Behavior of Aqueous Nanosized Zinc Oxide Suspensions. Journal of the American Ceramic Society, 2002, 85, 2161-2165.	3.8	74
151	Sintering and Ionic Conductivity of CuO-Doped Tetragonal ZrO2 Prepared by Novel Colloidal Processing Journal of the Ceramic Society of Japan, 2001, 109, 1004-1009.	1.3	6
152	Dense, bubble-free ceramic deposits from aqueous suspensions by electrophoretic deposition. Journal of Materials Research, 2001, 16, 321-324.	2.6	91
153	Sintering Characteristics of Iron Ultrafine Powders. Solid State Phenomena, 1992, 25-26, 179-186.	0.3	0
154	Fabrication of Highly Microstructure Controlled Ceramics by Novel Colloidal Processing. Key Engineering Materials, 0, 336-338, 2372-2377.	0.4	0
155	Pulsed-DC Electrophoretic Deposition (EPD) of Aqueous Alumina Suspension for Controlling Bubble Incorporation and Deposit Microstructure. Key Engineering Materials, 0, 412, 39-44.	0.4	10
156	Surface Modification of SiC Powder for Use in Electrophoretic Deposition. Key Engineering Materials, 0, 412, 287-290.	0.4	3
157	Textured PbTiO ₃ Based Ceramics Fabricated by Slip Casting in a High Magnetic Field. Key Engineering Materials, 0, 421-422, 395-398.	0.4	0
158	Control of Residual Stress in Multilayered Alumina Composites Prepared Using EPD in a Strong Magnetic Field. Key Engineering Materials, 0, 412, 233-236.	0.4	1
159	Preparation of Barium Titanate Grain-Oriented Ceramics and their Piezoelectric Properties. Key Engineering Materials, 0, 445, 3-6.	0.4	1
160	Textured Ti ₃ SiC ₂ by EPD in a Strong Magnetic Field. Key Engineering Materials, 0, 507, 15-19.	0.4	2
161	Textured Beta-Sialon:Eu ²⁺ Phosphor Deposits Fabricated by Electrophoretic Deposition (EPD) Process within a Strong Magnetic Field: Preparation Process and Photoluminescence (PL) Properties Depending on Orientation. Key Engineering Materials, 0, 654, 268-273.	0.4	0
162	Surface Modification of Complex Oxide Powder with Polyelectrolyte Layers Improving EPD Characteristics. Key Engineering Materials, 0, 654, 255-260.	0.4	0

#	Article	IF	CITATIONS
163	Fabrication of c-Axis-Oriented Zeolite L Seed Layer on Porous Zirconia Substrate by Electrophoretic Deposition in Strong Magnetic Field. Key Engineering Materials, 0, 654, 274-279.	0.4	0
164	ITO@SiO2 and ITO@{M6Br12}@SiO2 (M = Nb, Ta) Nanocomposite Films for Ultraviolet-Near Infrared Shielding. Nanoscale Advances, 0, , .	4.6	8
165	Tri-axial Grain Orientation of Y ₂ Ba ₄ Cu ₇ O _{<i>y</i>} Achieved by the Magneto-science Method. Applied Physics Express, 0, 1, 111701.	2.4	46
166	Fabrication of YSZ-Carbon Felt Composite Materials by Spark Plasma Sintering Process. Key Engineering Materials, 0, 904, 339-343.	0.4	0